Available online at www.sciencedirect.com
ScienceDirect
Thermochimica Acta 469 (2008) 28–35
thermochimica acta
www.elsevier.com/locate/tca

Experimental investigations on temperature-dependent thermo-physical and mechanical properties of pultruded GFRP composites

Yu Bai [a,1], Nathan L. Post [b,2], John J. Lesko [b,3], Thomas Keller [a,*]

[a] *Composite Construction Laboratory CCLab, Swiss Federal Institute of Technology EPFL, BP 2225, Station 16, CH-1015 Lausanne, Switzerland*
[b] *Department of Engineering Science & Mechanics, Virginia Polytechnic Institute & State University, 121A Patton Hall, MC 219, Blacksburg, VA 24061, USA*

Received 17 July 2007; received in revised form 24 December 2007; accepted 6 January 2008
Available online 16 January 2008

Abstract

The temperature-dependent thermo-physical and mechanical properties of a pultruded E-glass fiber-reinforced polyester (GFRP) composite are investigated in this paper. Fitting of theoretical models of the material properties to results of TGA, DSC, hot disk, and DMA experiments demonstrated good agreements. The constants for an Arrhenius representation of the decomposition mass-loss were determined using multi-curves methods. The effective specific heat capacity for the virgin material was found to increase during the decomposition process. A series model based on component volume fraction during decomposition provided an accurate description of the thermal conductivity as a function of temperature as measured by hot disk. Models based on the kinetic theory can describe the material degradation during glass transition as indicated by DMA results, while the parameters still need to be accurately identified. This paper provides a full set of temperature-dependent physical properties of a polyester matrix composite and demonstrates the applicability of theoretical models to represent the experimental results.

Keywords: Polymer–matrix composites; Thermogravimetry; Differential scanning calorimetry; Hot disk; Dynamic mechanical analysis

1. Introduction

Fiber-reinforced polymer (FRP) composites have been increasingly used in different fields, such as defense, aerospace, marine and civil engineering. Pultrusion is commonly used to produce FRP profiles with different structural shapes in an economic way. In many applications, these materials must withstand elevated temperatures while maintaining structural integrity. The temperature-dependent thermo-physical and mechanical properties of an E-glass/polyester composite material, including the specific heat capacity, thermal conductivity, mass transfer, storage and loss modulus and decomposition behavior are the focus of this paper. Due to the viscoelastic behavior of the polymer matrix in many composites, the physical properties of the composite can change drastically over relatively small changes in temperature [1,2]. Complicated processes occur at characteristic temperatures including the matrix glass transition and decomposition temperatures. The effective values of physical and mechanical properties are influenced by the chemical changes caused by increased temperature [3–5]. In order to estimate and predict the thermal responses of composite materials, it is necessary to evaluate and model the temperature-dependent thermo-physical and thermo-mechanical properties.

Experimental investigations were conducted by Henderson et al. on glass-filled phenol-formaldehyde (phenolic) resin composite: temperature-dependent mass-loss during decomposition was investigated by thermogravimetric method (TGA) in 1981 [3]. Multi-curves method (Friedman method) was used to identify the kinetic parameters in the Arrhenius equation. The temperature-dependent effective specific heat capacity (including the decomposition) was studied in 1982 by differential

* Corresponding author. Tel.: +41 216 933 227; fax: +41 216 936 240.
E-mail addresses: yu.bai@epfl.ch (Y. Bai), postnl@vt.edu (N.L. Post), jlesko@exchange.vt.edu (J.J. Lesko), thomas.keller@epfl.ch (T. Keller).
[1] Tel.: +41 216 936 263.
[2] Tel.: +1 540 231 3139; fax: +1 540 231 9187.
[3] Tel.: +1 540 231 5259; fax: +1 540 231 9187.

0040-6031/$ – see front matter © 2008 Elsevier B.V. All rights reserved.
doi:10.1016/j.tca.2008.01.002

Table 1
Fiber volume and weight fraction of pultruded 6 mm and 3 mm laminates

Sample	Fiber volume fraction (%)	Fiber weight fraction (%)
6 mm	35.6	57.6
3 mm	36.1	58.1

scanning calorimetry (DSC) [4,5]; and in 1983, the temperature-dependent thermal conductivity was obtained by line source technique [6]. In the recent work conducted by Lattimer and Quellette in 2006 [7], the temperature-dependent mass-loss, effective specific heat capacity, and thermal conductivity were investigated on glass fiber-reinforced vinyl ester composites (GFRP) from ambient temperature to 800 °C. Inverse heat transfer analysis was used to determine the thermo-physical properties by specifying the boundary condition of the samples as close to adiabatic as possible. Together with these experimentally obtained temperature-dependent thermo-physical properties, a thermal response model was also proposed in their work.

The temperature-dependent mass-loss due to decomposition was further investigated for various polymer and composite materials, such as bismaleimide resin by Regnier and Guibe [8], DGEBA/MDA system by Lee et al. [9], etc.

Overall, the reported experimental and modeling work conducted for the thermo-physical and thermo-mechanical properties of GFRP composites manufactured by pultrusion is very limited. This paper provides a complete experimental data set for temperature-dependent thermo-physical and mechanical properties of a pultruded GFRP composite. The experimental data was then used to further verify recently developed models for thermo-physical and mechanical properties [10,11].

2. Description of experimental materials

The pultruded GFRP laminates (provided by Fiberline A/S, Denmark) investigated in this study consisted of E-glass fibers embedded in an isophtalic polyester resin. The laminates had two different thicknesses (3 mm and 6 mm). Burn-off tests were performed to obtain the fiber mass content of the materials according to ASTM D3171-99 [12], the volume fraction was calculated considering a glass fiber density of 2.53 g/cm^3; the results are summarized in Table 1. Observation of the residual char material after a burn-off test showed that the laminate consisted of two mat layers sandwitching a layer of unidirectional roving. The mat layer of the 6 mm laminate consisted of a chopped strand mat (CSM) and a woven roving ply [0°/90°], both stitched together, while the 3 mm laminate contained only a CSM on each side. Microscopy was further used to obtain the details of the fiber architecture (see Fig. 1). For 3 mm laminates, the mat and rovings layers had an average thickness of 0.6 mm and 1.8 mm, respectively, while the 6 mm laminates exhibited 1.5 mm and 3.0 mm average thickness for mat and roving layers, respectively. The required sizes of the specimens used in the following experiments were cut or ground from these laminates.

3. Experimental investigation

3.1. Temperature-dependent mass change

The Thermogravimetric analysis method is widely accepted as a standard to investigate the mass change of polymer materials, including polymer matrix composites during the decomposition process [13]. The specimens were created by grinding the 6 mm laminate into a powder using a rasp. The material was taken through the entire laminate thickness to ensure that the fiber and resin contents of powder and laminate were the same. These specimens were analyzed by a TGA Q500 machine from TA Instruments, Inc. The tests were carried out from ambient temperature (25 °C) to 700 °C in an air atmosphere with a flow rate of 60 ml/min. Four heating rates (2.5, 5.0, 10.0, and 20.0 °C/min) were used. The initial mass of the specimens was 6.0 ± 0.3 mg for all runs. The experimental

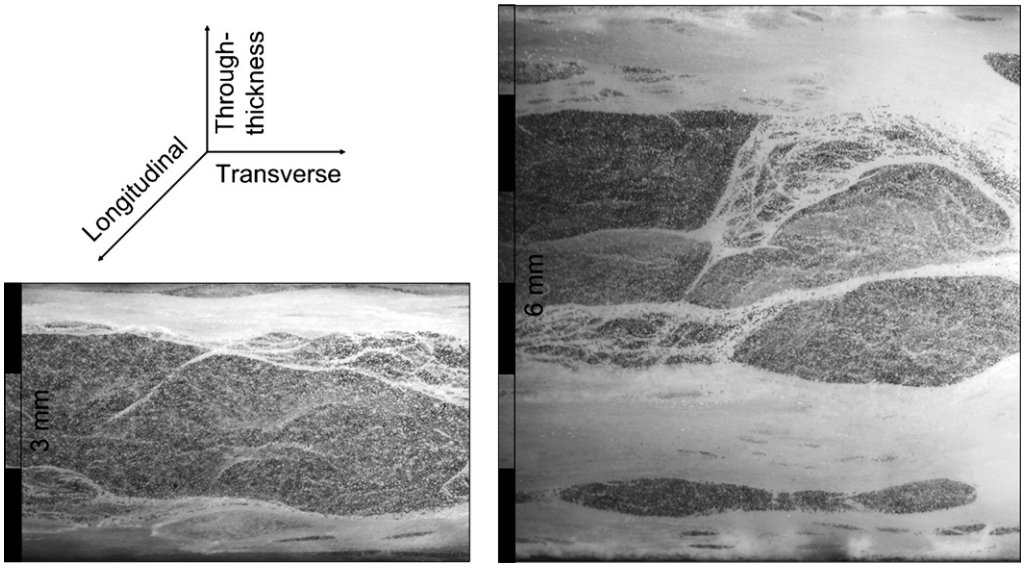

Fig. 1. Material architecture for pultruded 3mm (left) and 6mm (right) laminates by microscope.

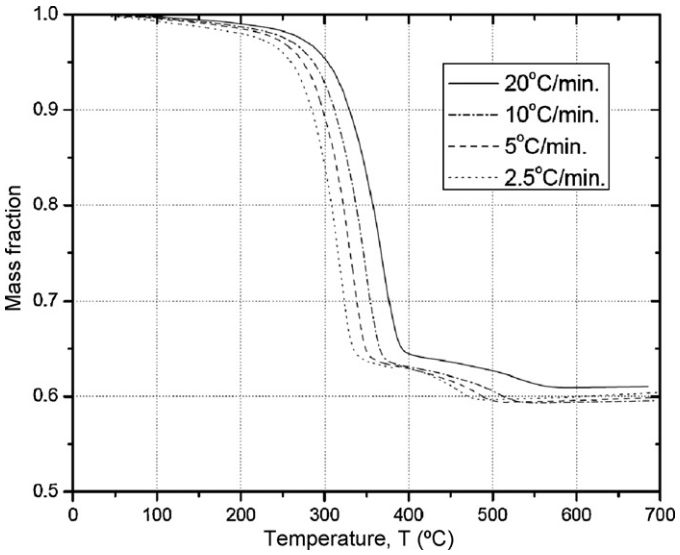

Fig. 2. Temperature-dependent mass fraction at different heating rates from TGA.

curves of mass fraction (temperature-dependent mass divided by the initial mass) are shown in Fig. 2.

3.2. Temperature-dependent specific heat capacity

Different methods can be used to obtain the specific heat capacity of the material at different temperatures, such as direct measurement by calorific method (ASTM C351), indirect measurement by transient hot wire method (ASTM C1113), transient line source (ASTM D5930-97), or laser flash (ASTM E1461-01). Differential Scanning Calorimetry (DSC), introduced in ASTM E1269 [14], was used as a direct measurement method in this paper.

For the DSC experiments, powder was ground from 6 mm laminates. Two specimens of virgin material (13.7 and 12.0 mg) were tested by a DSC analyzer (DSC Q1000, TA instrument, Inc.) from ambient temperature to 300 °C under a heating rate of 5 °C/min. Small specimen masses were used in order to reduce the temperature gradients in the material. During testing nitrogen atmosphere at a purge rate of 50 ml/min was maintained to prevent thermo-oxidative degradation. Under the same conditions, two specimens from char material (25.4 and 23.0 mg) obtained after burn-off experiments were tested. The resulting experimental curves for the temperature-dependent specific heat capacity (normalized with respect to the initial mass) of the virgin and char materials are shown in Fig. 3.

3.3. Temperature-dependent thermal conductivity

For measuring the temperature-dependent thermal conductivity, two different categories of analytical methods are available:

1. Steady heat flux analysis, such as (amongst others) guarded hot plate method (ASTM C177), or comparative longitudinal heat flow (ASTM E1225).
2. Transient heat flux analysis, such as transient hot wire method (ASTM C1113), or transient line source (ASTM D5930-97).

The hot disk method with transient thermal analysis was used in this case. This is an experimental technique developed using the concept of the transient hot strip (THS) technique, first introduced by Gustafsson [15]. The method is accepted as one of the most convenient techniques for studying thermal conductivity [16,17]. One advantage is that the apparatus employs a comparatively large specimen that allows analyzing the material in its proper structure rather than as a small non-representative coupon.

Only the through-thickness thermal conductivity was measured. The specimen used consisted of two 100 mm square plates of 6 mm thickness. The hot plate sensor was placed between the two plates and was then heated by an electrical current for a short period of time. The dissipated heat caused a temperature rise in both, the sensor and the surrounding specimen. The average temperature rise of the sensor was measured by recording the change of the electrical resistance. Resistivity changes with temperature and the temperature coefficient of resistivity (TCR) of the sensor material were determined in advance. By comparing the recorded transient temperature rise with that of the theoretical solution from the thermal conductivity equation, the thermal conductivity was determined.

Hot disk experiments (using a Hot Disk Thermal Constants Analyzer, manufactured by Hot Disk Inc.) were repeated three times on each virgin and char specimen at ambient temperature using a Kapton hot plate sensor which provides relatively high accuracy. Experiments at higher temperatures, up to 700 °C, were performed on both virgin and char material with a Mika hot plate sensor, which is of lower accuracy. The results from the Mika sensor were then calibrated to the Kapton sensor results at ambient temperature. All of these results are shown in Fig. 4.

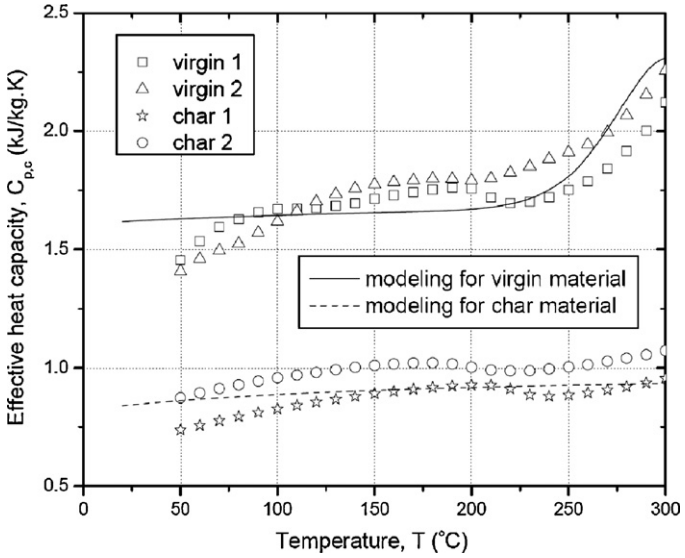

Fig. 3. Effective specific heat capacity on virgin and char materials as a function of temperature (normalized with respect to initial mass of sample) from DSC and modeling.

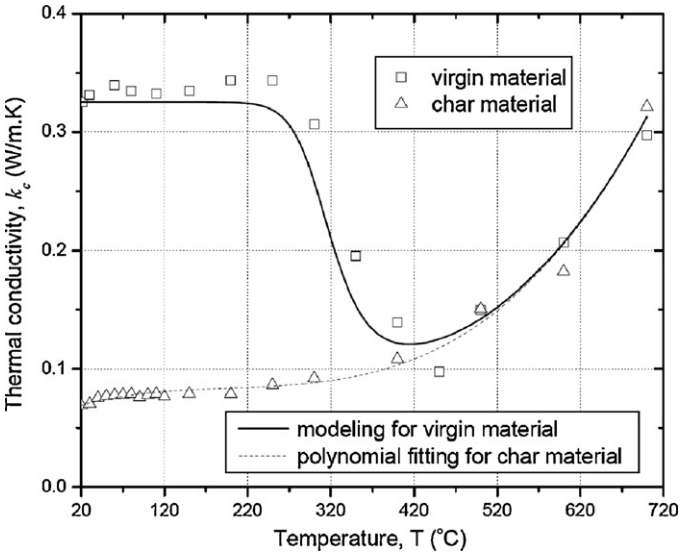

Fig. 4. Temperature-dependent effective thermal conductivity on virgin and char materials from hot disk experiments and modeling.

3.4. Temperature-dependent mechanical properties

In order to obtain the temperature-dependent elastic and viscoelastic mechanical properties of the material (storage and loss moduli), and to determine the kinetic parameters of the glass transition, DMA was conducted on specimens with 3 mm thickness (see Section 2 for material description). Considering the orthotropic characteristics of the composite materials, two specimens were cut from different directions (longitudinal and transverse, see Fig. 1). The resulting size was 50 mm long × 5 mm wide × 3 mm thick. Cyclic dynamic loads were imposed using a dual cantilever fixture on a DMA 2980 Dynamic Mechanical Analyzer from TA Instruments, Inc. The detailed procedure is according to ASTM D 5023-99 [18]. The specimens were ramped from room temperature to 250 °C at three different heating rates (2.5, 5 and 10 °C/min) and a dynamic oscillation frequency of 1 Hz. The specimen at 5 °C/min was cooled to room temperature and heated back to 250 °C two more times so that any changes from post-curing or thermal degradation could be noted. The results from different runs at 5 °C/min are shown in Fig. 5 for longitudinal direction (i.e. pultrusion direction) and Fig. 6 for transverse direction; the results for different heating rates for the longitudinal direction are shown in Fig. 7.

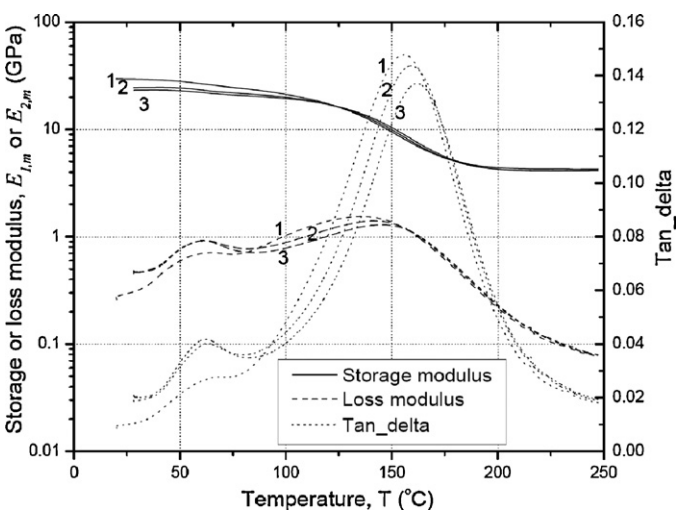

Fig. 5. Temperature-dependent storage modulus, loss modulus and tan-delta in longitudinal direction from three-run DMA (1–3: number of run).

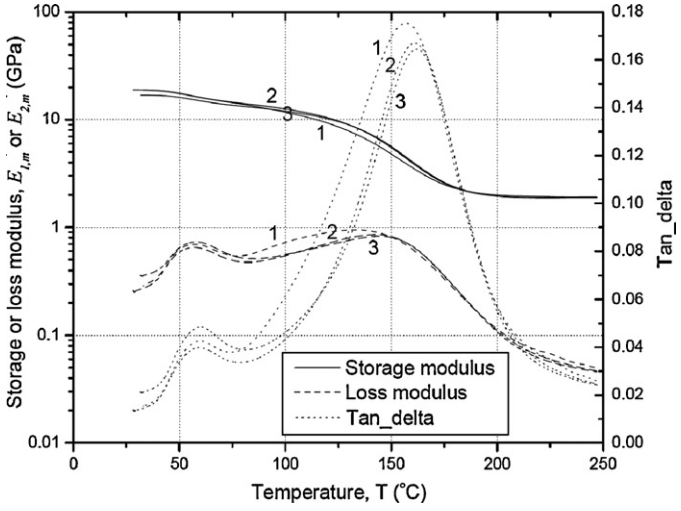

Fig. 6. Temperature-dependent storage modulus, loss modulus and tan-delta in transverse direction from three-run DMA (1–3: number of run).

4. Discussion and modeling

4.1. Temperature-dependent mass transfer

The temperature-dependent mass fraction curves from different heating rates are summarized in Fig. 2. The mass of the material did not change noticeably until the decomposition of the polyester resin started. The onset of decomposition temperature ($T_{d,onset}$) was determined as the temperature at which 5% of the mass was lost, and T_d was determined as the point when

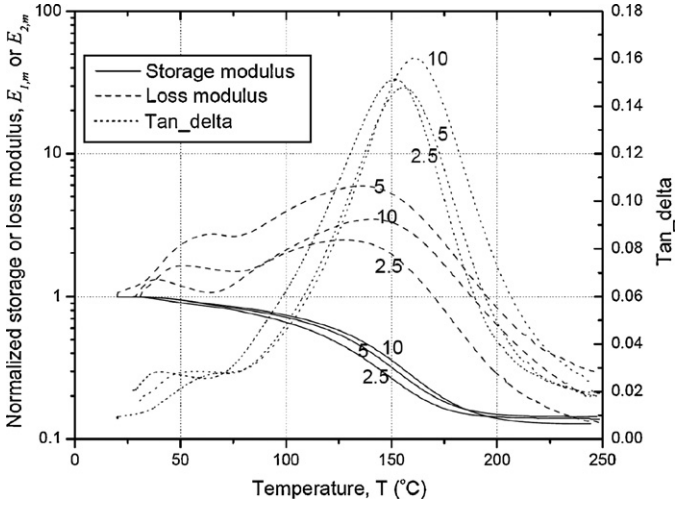

Fig. 7. Storage and loss modulus normalized by the initial values at 25 °C for each specimen, and tan-delta curves in longitudinal direction for three different heating rates (°C/min).

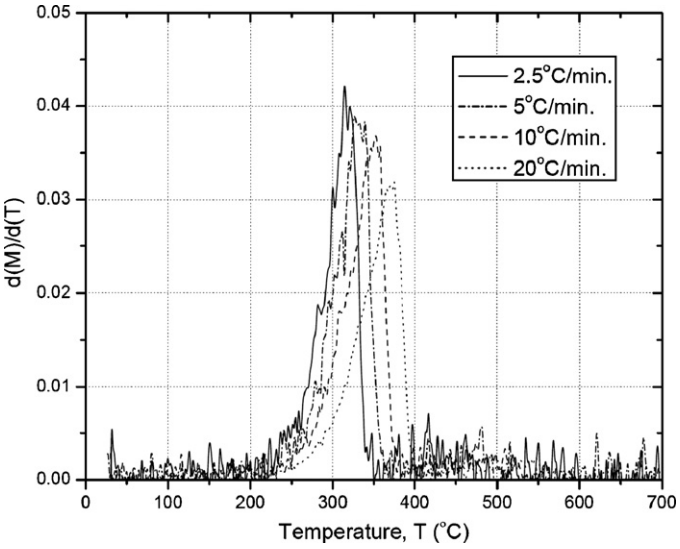

Fig. 8. Derivation curve of temperature-dependent mass for different heating rates.

the mass decreased at the highest rate, based on the derivative weight curve in Fig. 8. The results from different heating rates are summarized in Table 2. It can be seen that both, T_d and $T_{d,onset}$, increased with the increase of heating rate, because a lower heating rate corresponded to a longer heating time, and thus resulting in a more noticeable decomposition at a same temperature point. The residual mass fractions from all heating rates are around 60% (see Table 2) of the original material. Thus, considering the fiber mass fraction of 58% obtained by burn-off (see Table 1), most of the residual material in the TGA was glass fiber.

Simplifying decomposition of resin as one-step chemical process, this process can be modeled by the Arrhenius equation:

$$\frac{d\alpha_d}{dT} = \frac{A_d}{\beta} \cdot \exp\left(\frac{-E_{A,d}}{RT}\right) \cdot (1-\alpha_d)^n \quad (1)$$

where α_d is the conversion degree of decomposition, A_d is the pre-exponential factor, $E_{A,d}$ is the activation energy, and n is the reaction order. R is the universal gas constant (8.314 J/mol K), and β is a constant heating rate. The Ozawa method [19], as a multi-curves method, was used to identify the kinetic parameters (A_d, $E_{A,d}$ and n) and the results are summarized in Table 3. Substituting these parameters into Eq. (1), the theoretic conversion degrees of decomposition were obtained in Fig. 9 (only the curves at heating rates 20 °C/min and 2.5 °C/min are shown for better viewing), which compared well with the experimental results. However, some variations still were found between

Table 2
Decomposition temperatures $T_{d,onset}$, T_d and residual mass from TGA tests at different heating rates

Heating rate (°C/min)	$T_{d,onset}$ (°C)	T_d (°C)	Residual mass (%)
20	304	371	61.0
10	287	353	59.6
5	274	337	59.9
2.5	260	321	60.4

Table 3
Kinetic parameters for glass transition and decomposition

Transition	Activation energy E_A (J/mol)	Pre-exponential factor, A (min^{-1})	Reaction order, n
Glass (Ozawa)	118,591	2.49×10^{15}	1.89
Glass (Kissinger)	131,387	3.24×10^{16}	0.86
Decomposition (Ozawa)	124,953	2.72×10^{10}	2.75

350 °C and 400 °C. Considering that decomposition is a complicated process and different elemental reactions are involved, a single equation cannot entirely described all the concurrent processes. It seems that the decomposition can be better described if separating it as a two-stage process [3]; however, the problem of identifying the kinetic parameters from two coupled processes remains a challenge in such an approach.

4.2. Temperature-dependent heat capacity

As shown in Fig. 3, when the temperature is lower than 250 °C, the increase of the specific heat capacity of the virgin material is very small; in fact, theoretically, the specific heat capacity of pure resin or fibers increases with temperature based on the classic Einstein or Debye model. When the temperature is close to 275 °C ($T_{d,onset}$ is 274 °C at a heating rate of 5 °C/min, see Table 2), the effective heat capacity of the virgin material started to increase faster, because the decomposition process is an endothermic chemical reaction. Similar experimental results also can be found for glass-filled phenol-formaldehyde resin composite in [5], and for E-glass fiber vinyl ester in [7]. The change of the DSC curve of the char material is very small when temperature is increased up to 300 °C, since it mainly consisted of glass fibers.

The model for temperature-dependent effective specific heat capacity, normalized to the initial mass, $C_{p,c}$, and proposed in

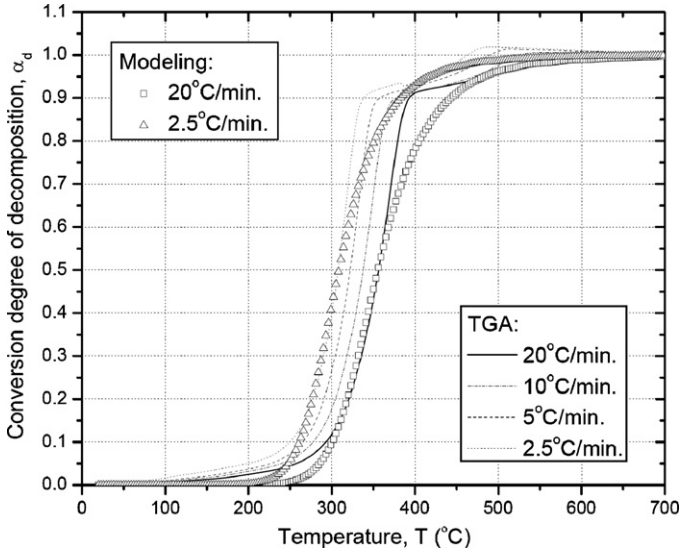

Fig. 9. Conversion degrees of decomposition at different heating rates from TGA; comparison to results from Ozawa method.

[10], can be expressed as:

$$C_{p,c} = C_{p,b} \cdot (1 - \alpha_d) + C_{p,a} \cdot \frac{M_e \cdot \alpha_d}{M_i} + \frac{d\alpha_d}{dT} \cdot C_d \quad (2)$$

where $C_{p,b}$ and $C_{p,a}$ are the specific heat capacity of the virgin and decomposed char material in kJ/kg K. M_i and M_e are the initial and final mass. C_d is the total decomposition heat in kJ/kg, α_d as obtained in Section 4.1.

The modeling curve for true specific heat capacity of char material ($C_{p,a}$) was calculated based on the model in [10], and comparing with the DSC curve on char material in Fig. 3, a good agreement was found. Substituting the theoretic curve of $C_{p,a}$ into Eq. (2), and taking the value at 100 °C from the DSC curve of virgin material as $C_{p,b}$, the model curve of the specific heat capacity of the virgin material can be obtained. The comparison with the DSC results on virgin material is shown in Fig. 3. The increase of heat capacity due to decomposition is well described by this model; while there is still a small increment of heat capacity from the initial temperature to around 100 °C that remains unaccounted for in the model. This difference could be due to the fact that the true specific heat capacity of pure material (for example, pure polyester) is increasing with temperature or because of measurement inaccuracy in the initial stage of temperature increase. Similar results also can be found in DSC results on E-glass fiber vinyl ester in [7]. Since the highest temperature achieved in the experiments was only 300 °C, the decomposition process was not fully covered; the theoretic curve in the higher temperature range should be further confirmed, as well as the total decomposition heat, C_d.

4.3. Temperature-dependent thermal conductivity

The thermal conductivity measured for virgin and char material at room temperature are 0.325 ± 0.004 and 0.069 ± 0.002 W/m K, respectively. Char material has a much lower thermal conductivity at room temperature since the resin has already decomposed; gaps and voids are left in the composite between the glass fibers that significantly increase the thermal resistance (shielding effects, see [10]).

The thermal conductivity measured at different temperatures for both virgin and char material are shown in Fig. 4. The thermal conductivity of the char material (mostly glass fibers) increased with the temperature, because the thermal conductivity of glass fibers also increases at these temperatures.

The change of thermal conductivity of the virgin material is comparatively small when temperature is lower than 280 °C (i.e. before the decomposition of the resin), while a strong decrease is apparently when the temperature is approaching T_d due to shielding effects of emerging voids [10]. When the resin is fully decomposed, the temperature-dependent thermal conductivity curve approaches and follows that of the char material.

At any specified temperature, the composite material can be considered as a material composed of two phases: the virgin material and the decomposed char material, which are connected in series in the heat flow (through-thickness) direction. The effective thermal conductivity of the composite materials can then be obtained as

$$\frac{1}{k_c} = \frac{V_b}{k_b} + \frac{V_a}{k_a} \quad (3)$$

where V_b and V_a are the volume fractions of the virgin material and decomposed char material, which can be expressed as [10]

$$V_b = 1 - \alpha_d \quad (4)$$

$$V_a = \alpha_d \quad (5)$$

Considering k_b as the thermal conductivity of the virgin material at room temperature (0.325 W/m K), and k_a as the curve of temperature-dependent thermal conductivity of char material in Fig. 4, the model curve of the virgin material was obtained. The comparison with the experimental data in Fig. 4 shows a good agreement. It should be noted that the time-dependent temperature progression (a constant heating rate, for example) is necessary to determine the conversion degree of decomposition, α_d (see Section 4.1). As this information was not available in the high temperature hot disk experiments, the temperature-dependent α_d obtained at 20 °C/min (in Section 4.1) was used in Eqs. (4) and (5) to estimate the volume fractions of the different phases at different temperatures. This comparatively high rate was adopted in view of the rapid heating of the hot disk oven system.

Table 4
Glass transition temperature T_g and $T_{g,onset}$ by DMA tests from different runs and for different directions

Run	$T_{g,onset}$		T_g	
	Longitudinal (°C)	Transverse (°C)	Longitudinal (°C)	Transverse (°C)
1	112	112	156	157
2	116	118	159	161
3	124	123	162	162

4.4. Temperature-dependent mechanical properties

As shown in Figs. 5 and 6, for both longitudinal and transverse directions, the storage modulus monotonically decreased with the increasing of temperature, with the highest rate of change occurring between 145 °C and 165 °C. The glass transition temperature, T_g (determined by the peak point of the tan-delta curve), and the $T_{g,onset}$ are summarized in Table 4 for different runs of the specimens in different directions. It can be seen that the resulting T_g from the two different directions is very similar, because the temperature effects mainly depend on the polyester resin, which was the same. On the other hand, three-run DMA tests on the same specimen showed that T_g is slightly increased with the number of runs for both directions (see Table 4). The curves of storage and loss modulus from different runs, however, are almost the same, thus post-curing effects were not observed. As also reported by the profile manufacturer, 180 °C was reached during the pultrusion process and thus full curing must have been already achieved. It should be noted that a small peak before glass transition was found for the loss modulus and tan-delta

Table 5
Storage and loss moduli for different material states in two different directions

Material state	Storage modulus, E_1 (GPa)	
	Longitudinal	Transverse
Glassy	29.6	18.9
Rubbery	4.26	1.91

curves in all runs and in both directions (see Figs. 5 and 6). This could result from secondary relaxations of the polymer resin [20] or from additives. DMA results from different heating rates showed similar behavior, as shown in Fig. 7 where the storage and loss modulus were normalized by their initial room temperature values for each specimen. Faster heating rates delay the temperature of glass transition noted by the right shift of the storage modulus curves and the peaks of tan-delta and loss modulus curves.

The glass transition can be modeled by the Arrhenius equations [11]:

$$\frac{d\alpha_g}{dT} = \frac{A_g}{\beta} \cdot \exp\left(\frac{-E_{A,g}}{RT}\right) \cdot (1-\alpha_g)^n \quad (6)$$

where α_g is the conversion degree, A_g is the pre-exponential factor, $E_{A,g}$ is the activation energy (which is considered as a constant for one specified process) for glass transition. The Ozawa method [19] and Kissinger method [21] were used to determine the kinetic parameters based on the curves from three different heating rates. The corresponding kinetic parameters are summarized in Table 3.

Knowing the degree of conversion for the different transitions from Eq. (6), the temperature-dependent storage modulus, $E_{1,m}$ of FRP composite materials can be calculated as:

$$E_{1,m} = E_{1,g} \cdot (1-\alpha_g) + E_{1,r} \cdot \alpha_g \quad (7)$$

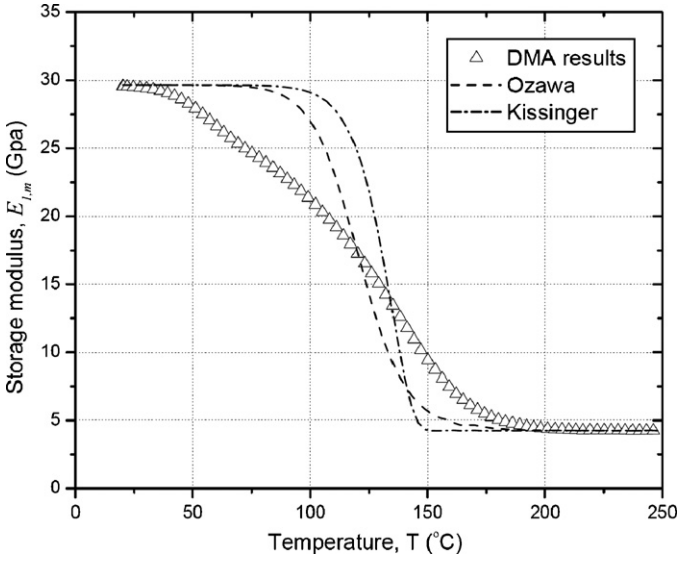

Fig. 10. Comparison of experimental and modeling curves of temperature-dependent storage modulus in longitudinal direction (at 5 °C/min).

where $E_{1,g}$ and $E_{1,r}$ are the storage moduli in glassy state and rubbery state, respectively. These values are obtained based on the DMA (see Section 3.4) and are summarized in Table 5. It was found that the storage moduli in glassy state obtained by DMA for both longitudinal and transverse directions are very similar to the corresponding values of elastic modulus reported in [22]. The mechanical properties are considered as zero for the decomposed state.

The modeling curves of temperature-dependent storage modulus, resulting from the Ozawa and Kissinger methods, are shown in Fig. 10 for the longitudinal direction (at 5 °C/min). The discrepancy between the modeling and experimental results could be attributed to the inaccuracy of the methods for the kinetic parameter estimation, or because of the E_A-dependencies induced by multi-step kinetics of the process. Different methods for kinetic parameters identification were discussed and compared in detail in [23–27], and an error analysis was presented in [28]. These methods are mainly used for the kinetic analysis of the decomposition process and seldom for the analysis of glass transition. It is apparent that the application of these methods to obtain kinetic parameters for glass transition requires further investigation.

5. Conclusions

For the further understanding and application of pultruded GFRP composites under elevated and high temperatures, a series of experiments were conducted to investigate the temperature-dependent thermo-physical and mechanical properties, including the mass-loss, specific heat capacity, thermal conductivity, and storage and loss modulus. The following conclusions were obtained:

(1) The mass of the composite material is stable before T_d. When the decomposition is approaching, the mass starts to decrease rapidly. The Arrhenius equation can be used to model the decomposition process; multi-curves methods were used to identify the kinetic parameters. Further investigation could be involved in the feasibility of characterizing decomposition behavior by multi-stage chemical reactions.
(2) The change of specific heat capacity of the composite material is not very significant when the temperature is below T_d. However, the measured value rapidly increases during the decomposition process because additional heat is required for this endothermic chemical reaction. This behavior can be well modeled with the concept of effective specific heat capacity. However, measurements over a higher temperature range would be desirable to cover the whole decomposition process, and to further verify the total decomposition heat.
(3) The thermal conductivity of fully decomposed material is much lower than that of virgin material at room temperature. For decomposed material, thermal conductivity was seen to increase with temperature. For virgin material, the effective thermal conductivity is decreased when decomposition occurs, since shielding effects are induced by emerging voids filled with gases from the decomposed resin. The effective thermal conductivity can be accurately described

by a series model whereby the volume fraction of different phases can be obtained from the decomposition model.

(4) The storage modulus of the composite material decreased, while the loss modulus increased, with increasing temperature. The rates accelerate when temperature is approaching T_g. However, when temperature exceeds T_g, the loss modulus starts to decrease. The temperature-dependent mechanical properties show similar behavior in both longitudinal and transverse directions. The Arrhenius equation was used to describe the glass transition. However, the estimation of the kinetic parameters for glass transition using existing multi-curves methods led to inaccurate results and further investigation is warranted.

Acknowledgements

The authors would like to acknowledge the support of the Swiss National Science Foundation (Grant No. 200020-109679/2), Fiberline Composites A/S, Denmark for providing the experimental materials, and, John Bausano, Jason Cain and Dr. Aixi Zhou at Virginia Tech for supporting the experiments.

References

[1] A.S. Hilal, A.M. Abousehly, M.T. Dessouky, M.T.A.A.A.B.D. El-hakim, J. Appl. Polym. Sci. 49 (1993) 559–563.
[2] M.R. Tant, Proceedings of the ACS Symposium Series 603, San Diego, CA, USA, 1994.
[3] J.B. Henderson, M.R. Tant, G.R. Moore, J.A. Wiebelt, Thermochim. Acta 44 (1981) 253–264.
[4] J.B. Henderson, J.A. Wiebelt, M.R. Tant, G.R. Moore, Thermochim. Acta 57 (1982) 161–171.
[5] J.B. Henderson, Thermochim. Acta 131 (1988) 7–14.
[6] J.B. Henderson, Y.P. Verma, M.R. Tant, G.R. Moore, Polym. Comp. 4 (1983) 219–224.
[7] B.Y. Lattimer, J. Quellette, Comp. Part A 37 (2006) 1068–1081.
[8] N. Regnier, C. Guibe, Polym. Degrad. Stab. 55 (1997) 165–172.
[9] L.Y. Lee, M.J. Shim, S.W. Kim, J. Appl. Polym. Sci. 81 (2001) 479–485.
[10] Y. Bai, T. Vallée, T. Keller, Comp. Sci. Technol. (2007) 3098–3109.
[11] Y. Bai, T. Keller, T. Vallée, Comp. Sci. Technol., under review.
[12] ASTM D3171-99 Standard Test Method for constituent content of composite materials.
[13] ASTM E1131-03 Standard Test Method for compositional analysis by Thermogravimetry.
[14] ASTM E1269-01 Standard Test Method for Determining Specific Heat Capacity by Differential Scanning Calorimetry.
[15] S.E. Gustafsson, Rev. Sci. Instrum. 62 (1991) 797–804.
[16] Y. Jannot, P. Meukam, Meas. Sci. Technol. 15 (2004) 1932–1938.
[17] P. Mo, P. Hu, J. Cao, Z. Chen, H. Fan, F. Yu, Int. J. Thermophys. 27 (2006) 304–313.
[18] ASTM D5023-99 Standard Test Method for measuring the dynamic mechanical properties of plastics using three-point bending.
[19] T. Ozawa, Bull. Chem. Soc. Jpn. 38 (1965) 1881–1886.
[20] M.F. Ashby, D.R.H. Jones, Engineering Materials 2: An Introduction to Microstructures, Processing, and Design, Pergamon Press, Oxford, 1997.
[21] H.E. Kissinger, Anal. Chem. 29 (1957) 1702–1706.
[22] T. Keller, H. Gürtler, Comp. Struct. 70/4 (2005) 484–496.
[23] M.E. Brown, M. Maciejewski, S. Vyazovkin, Thermochim. Acta 355 (2000) 125–143.
[24] M. Maciejewski, Thermochim. Acta 355 (2000) 145–154.
[25] S. Vyazovkin, Thermochim. Acta 355 (2000) 155–163.
[26] A.K. Burnham, Thermochim. Acta 355 (2000) 165–170.
[27] S. Vyazovkin, C.A. Wight, Thermochim. Acta 340–341 (1999) 53–68.
[28] M.J. Starink, Thermochim. Acta 404 (2003) 163–176.